CONTROL OF CRITICAL COUPLING IN 3X3 MMI COUPLERS BASED ON OPTICAL MICRO-RING RESONATORS AND APPLICATIONS TO SELECTIVE WAVELENGTH SWITCHING, MODULATION, AMPLIFICATION AND OSCILLATION

Trung-Thanh Le

International School, Vietnam National University, Hanoi (VNU-IS); thanh.le@vnu.edu.vn

Abstract - Micro-ring resonator using 3x3 Multimode Interference (MMI) couplers or 3x3 planar directional coupler is a promising component for a new generation of functional optic devices such as switches, modulators and laser oscillators, which employ smaller applied voltages for control. In order to achieve these functional devices, means for voltage control of the coupling between the waveguides and the resonator is required. This paper presents a method of controlling the coupling coefficients to meet the critical coupling of 3x3 micro-ring resonator applied to optical switching, modulation and oscillation.

Key words - Integrated optics; Coupled resonators; Multimode Interference Couplers

1. Introduction

Micro-ring resonator is a promising device for applications in the field of optical communications. Using this structure, basic signal processing functions such as wavelength filtering, routing, switching, modulation, and multiplexing can be achieved [1]. However, most racetrack resonators have been designed and fabricated using directional couplers or 2x2 MMI couplers as a coupling element between the ring and the bus waveguides. Recently, we have been proposed a novel configuration of a micro-ring resonator using 3x3 MMI couplers [2, 3]. Devices using this structure hold the promise of a new generation of light switching, amplification, laser oscillation, and modulation.

Before this can proceed to real applications, we need to find out the mechanism to control the coupling coefficients precisely. One of the most interesting features is that the resonators operate at resonance wavelength and thus critical coupling can be achieved. This is the purpose of the present paper, in which we propose a configuration for precisely controlling the coupling coefficients of the coupler by using electro-optic or thermo-optic effect. The analysis of the device is based on self-imaging theory and transfer matrix method. Performance parameters are discussed.

From the research by A. Yariv about the modelling of micro-ring resonator based on 2x2 directional coupler as a matrix, this model is particularly important and used widely in analysis of optical circuits based on 2x2 micro-ring resonators [4, 5]. This research is to present an analysis and modelling of micro-ring resonators based on 3x3 MMI (multimode interference) and 3x3 planar directional coupler. Both structures are suitable for integrated optical circuits and a versatile functional device can be created from these structures.

In the literature, 3x3 fiber based resonators have been proposed and some applications based on this structure have been presented [6-10]. However, such analysis is not applicable to general applications. Here, we present an universal analysis applied for both 3x3 MMI and 3x3 planar directional coupler based micro-ring resonators.

2. Theory

A micro-ring resonator based on a 3x3 coupler is proposed in Fig. 1 below. It consists of lossless coupling between two optical waveguides and a ring resonator. The 3x3 coupler in this paper is made from a 3x3 MMI coupler. Compared to 3x3 fibre couplers or planar couplers, 3x3 MMI couplers have the advantage of the relaxed fabrication tolerances and the ease of integration of these devices into more complex photonic integrated circuits, small size, and low excess loss. Therefore, the use of 3x3 MMI couplers in micro-ring resonator configurations not only takes these advantages, but also precisely designs the desired couplers.

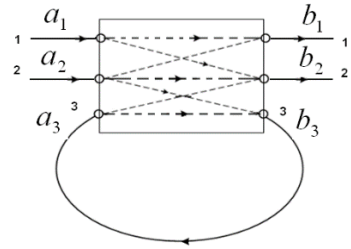

Figure 1. *Geometry of micro-ring resonator using a 3x3 coupler*

As given in [5], by controlling the coupling coefficients of the coupler to meet the critical coupling, small changes in the internal loss for a given coupling coefficient, or vice versa, can control the transmitted power, between unity and zero. Therefore, switching and modulation functions can be realized from this characteristic if we know how to control these parameters. Moreover, if we include a gain (optical amplifier) inside the ring resonator, the transmitted power can reach infinite value if the relation between the internal loss and coupling coefficient meet certain particular conditions.

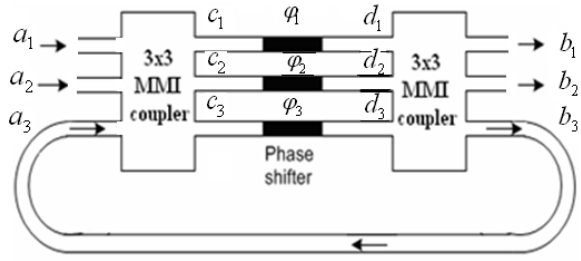

Figure. 2 *Geometry of microring resonator using a 3x3 coupler*

The proposed configuration for the control of the coupling coefficients is shown in Figure 2. It consists of a

generalized Mach–Zehnder interferometer (MZI) sandwiched between two 3x3 MMI couplers into the ring resonator. The MZI introduces the phase shifts φ_i (i=1-3) in its three arms.

Using the self-imaging theory, the 3x3 MMI coupler can be described by a transfer matrix [11]

$$M=\begin{pmatrix} \frac{1}{\sqrt{3}}e^{j(\theta+11\pi/24)} & \frac{1}{\sqrt{3}}e^{j(\theta-13\pi/24)} & \frac{1}{\sqrt{3}}e^{j(\theta-5\pi/24)} \\ \frac{1}{\sqrt{3}}e^{j(\theta-13\pi/24)} & \frac{1}{\sqrt{3}}e^{j(\theta-5\pi/24)} & \frac{1}{\sqrt{3}}e^{j(\theta-13\pi/24)} \\ \frac{1}{\sqrt{3}}e^{j(\theta-5\pi/24)} & \frac{1}{\sqrt{3}}e^{j(\theta-13\pi/24)} & \frac{1}{\sqrt{3}}e^{j(\theta+11\pi/24)} \end{pmatrix} \quad (1)$$

where θ is a constant phase, $\theta=-\beta_0 L_{MMI}+\frac{9\pi}{24}$, β_0 is the constant propagation of the fundamental mode within the MMI region, and L_{MMI} is the length of the MMI coupler, $L_{MMI}=L_\pi=\frac{4n_r W^2}{3\lambda}$; n_r, W, λ are refractive index of the core, width of the MMI coupler, and optical waveguide respectively; L_π is the beat length of the two lowest order modes in the MMI region.

The field $c_i\,(i=1\div3)$ at the output of the MMI coupler can therefore be related to the input field $a_i\,(i=1\div3)$ by the following matrix equations

$$\begin{pmatrix} c_1 \\ c_2 \\ c_3 \end{pmatrix} == M \begin{pmatrix} a_1 \\ a_2 \\ a_3 \end{pmatrix}, \text{ and } \begin{pmatrix} b_1 \\ b_2 \\ b_3 \end{pmatrix} == M \begin{pmatrix} d_1 \\ d_2 \\ d_3 \end{pmatrix} \quad (2)$$

The overall transfer matrix S of the MMI-GMZ structure shown in Fig. 2 is found from the product of the transfer matrices of the MMI splitter, the phase shifters, and the MMI combiner, and can therefore be written as [12]

$$S = M\Phi M \quad (3)$$

where M is the transfer matrix for each MMI coupler and Φ is the matrix due to the phase shifters

$$\Phi = \mathrm{diag}\left\{e^{j\phi_1}, e^{j\phi_2}, e^{j\phi_3}\right\} \quad (4)$$

Using (1) and (2) in (3) lead to the transmission expressions at the output port 1, P_{b_1} and port 2, P_{b_2} respectively

$$P_{b_1}=\left|s_{11}+\frac{s_{13}s_{31}\alpha e^{j\varphi}}{1-s_{33}\alpha e^{j\varphi}})a_1+(s_{12}+\frac{s_{13}s_{32}\alpha e^{j\varphi}}{1-s_{33}\alpha e^{j\varphi}})a_2\right|^2 \quad (5)$$

$$P_{b_2}=\left|(s_{21}+\frac{s_{23}s_{31}\alpha e^{j\varphi}}{1-s_{33}\alpha e^{j\varphi}})a_1+(s_{22}+\frac{s_{23}s_{32}\alpha e^{j\varphi}}{1-s_{33}\alpha e^{j\varphi}})a_2\right|^2 \quad (6)$$

Therefore, we obtain the transmitted powers at output ports when the input signal entering from port 1only ($a_2=0$) is as follows

$$P_1=\left|(s_{11}+\frac{s_{13}s_{31}\alpha e^{j\varphi}}{1-s_{33}\alpha e^{j\varphi}})\right|^2 \quad (7)$$

$$P_2=\left|(s_{21}+\frac{s_{23}s_{31}\alpha e^{j\varphi}}{1-s_{33}\alpha e^{j\varphi}})\right|^2 \quad (8)$$

And the transmitted powers at output ports when the input signal entering from port 2 ($a_1=0$) are

$$P_3=\left|s_{12}+\frac{s_{13}s_{32}\alpha e^{j\varphi}}{1-s_{33}\alpha e^{j\varphi}}\right|^2 \quad (9)$$

$$P_4=\left|s_{22}+\frac{s_{23}s_{32}\alpha e^{j\varphi}}{1-s_{33}\alpha e^{j\varphi}}\right|^2 \quad (10)$$

Without loss of generality, it is assumed that the optical waveguides support only one mode-the fundamental one and that the coupling is lossless, the relationship between output complex amplitudes and input complex amplitudes of the device can be described by using a coupling matrix as follows

$$\begin{pmatrix} b_1 \\ b_2 \\ b_3 \end{pmatrix} = \begin{pmatrix} \tau_{11} & \kappa_{12} & \kappa_{13} \\ \kappa_{21} & \tau_{22} & \kappa_{23} \\ \kappa_{31} & \kappa_{32} & \tau_{33} \end{pmatrix} \begin{pmatrix} a_1 \\ a_2 \\ a_3 \end{pmatrix} = M \begin{pmatrix} a_1 \\ a_2 \\ a_3 \end{pmatrix} \quad (1)$$

$$a_3 = \alpha \exp(j\varphi) b_3 \quad (2)$$

Where τ_{ij}, $\kappa_{ij}\,(i,j=1\div3)$ are transmission and coupling coefficients of power from input ports *i* to output ports *j;* $\alpha=\exp(-\alpha_0 L)$ is the transmission loss inside the resonators, and α_0 (dB/cm) is the loss coefficient in the core of the optical waveguides. $\varphi=\beta L$ is the phase accumulated over the ring waveguides with propagation constants β, where $\beta=2\pi n_{eff}/\lambda$, n_{eff} and λ are effective refractive index of the waveguide core and optical wavelength, respectively. The conservation of energy principle results in the equivalent conditions: M^*M and MM^* are unit matrices. Therefore, we have the following equations

$$|\tau_{11}|^2+|\kappa_{21}|^2+|\kappa_{31}|^2=1 \quad (3)$$

$$|\kappa_{12}|^2+|\tau_{22}|^2+|\kappa_{32}|^2=1 \quad (4)$$

$$|\kappa_{13}|^2+|\kappa_{23}|^2+|\tau_{33}|^2=1 \quad (5)$$

The field amplitudes are normalised to the input amplitudes a_1 (or a_2), that means we can choose $a_1=1$ (or $a_2=1$). The transmission around the ring is then calculated by

$$b_1=(\tau_{11}+\frac{\kappa_{13}\kappa_{31}\alpha e^{j\varphi}}{1-\tau_{33}\alpha e^{j\varphi}})a_1+(\kappa_{12}+\frac{\kappa_{13}\kappa_{32}\alpha e^{j\varphi}}{1-\tau_{33}\alpha e^{j\varphi}})a_2 \quad (6)$$

$$b_2=(\kappa_{21}+\frac{\kappa_{23}\kappa_{31}\alpha e^{j\varphi}}{1-\tau_{33}\alpha e^{j\varphi}})a_1+(\kappa_{22}+\frac{\kappa_{23}\kappa_{32}\alpha e^{j\varphi}}{1-\tau_{33}\alpha e^{j\varphi}})a_2 \quad (7)$$

From (6) and (7), we obtain the transmitted powers at output ports when the input signal entering from port 1($a_2 = 0$)is as follows

$$P_1 = \left| (\tau_{11} + \frac{\kappa_{13}\kappa_{31}\alpha e^{j\varphi}}{1-\tau_{33}\alpha e^{j\varphi}}) \right|^2 \quad (8)$$

$$P_2 = \left| (\kappa_{21} + \frac{\kappa_{23}\kappa_{31}\alpha e^{j\varphi}}{1-\tau_{33}\alpha e^{j\varphi}}) \right|^2 \quad (9)$$

And the transmitted powers at output ports when the input signal entering from port 2($a_1 = 0$) are

$$P_3 = \left| \kappa_{12} + \frac{\kappa_{13}\kappa_{32}\alpha e^{j\varphi}}{1-\tau_{33}\alpha e^{j\varphi}} \right|^2 \quad (10)$$

$$P_4 = \left| \kappa_{22} + \frac{\kappa_{23}\kappa_{32}\alpha e^{j\varphi}}{1-\tau_{33}\alpha e^{j\varphi}} \right|^2 \quad (11)$$

As an example, we consider the former case in this paper. (8) and (9) can be rewritten in the following forms:

$$P_1 = \left| \frac{|\tau_{11}|e^{j\phi_{11}} + (|\kappa_{13}||\kappa_{31}|e^{j(\phi_{13}+\phi_{31})} - |\tau_{33}||\tau_{11}|e^{j(\phi_{11}+\phi_{33})})\alpha e^{j\varphi}}{1-|\tau_{33}|\alpha e^{j(\varphi+\phi_{33})}} \right|^2 \quad (12)$$

$$P_2 = \left| \frac{|\kappa_{21}|e^{j\phi_{21}} + (|\kappa_{13}||\kappa_{23}|e^{j(\phi_{23}+\phi_{31})} - |\tau_{33}||\kappa_{21}|e^{j(\phi_{21}+\phi_{33})})\alpha e^{j\varphi}}{1-|\tau_{33}|\alpha e^{j(\varphi+\phi_{33})}} \right|^2 \quad (13)$$

Here $\phi_{ij}\,(i,j=1\div 3)$ are the phases of coupling coefficients. Most of the interesting features of this resonator occur near resonance $\varphi+\phi_{33}=2\pi m$, where m is integer. At resonance the transmitted powers at output ports 1 and 2 only depend on the loss inside micro-ring resonator and coupling coefficients.

$$P_1 = \left| \frac{|\tau_{11}|e^{j\phi_{11}} + \alpha(|\kappa_{13}||\kappa_{31}|e^{j(\phi_{13}+\phi_{31}-\phi_{33})} - |\tau_{33}||\tau_{11}|e^{j\phi_{11}})}{1-|\tau_{33}|\alpha} \right|^2 \quad (14)$$

$$P_2 = \left| \frac{|\kappa_{21}|e^{j\phi_{21}} + \alpha(|\kappa_{13}||\kappa_{23}|e^{j(\phi_{23}+\phi_{31}-\phi_{33})} - |\tau_{33}||\kappa_{21}|e^{j\phi_{21}})}{1-|\tau_{33}|\alpha} \right|^2 \quad (15)$$

One of the most special characteristics is that when a special relation between the internal loss and coupling coefficients is achieved, the power at output port 1 or output port 2 will vanish and this condition is called *critical coupling* condition as well-known in the microwave field [13]. The useful characteristics of the device such as switching, modulation and laser oscillation can be obtained from this condition.

3. Simulation results and discussions

As an example, we consider a ring resonator based on a 3x3 planar waveguide coupler only. The configuration of the ring resonator using a 3x3 coupler is shown in Figure 3.

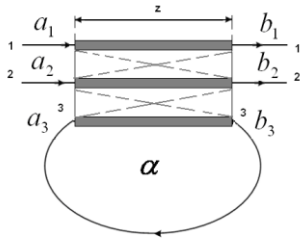

Figure 3. *Micro-ring resonator using a 3x3 planar coupler*

It is noted that our general theory can be applied to micro-ring resonator based on any kind of 3x3 couplers formed from 3x3 planar optical waveguides or 3x3 multimode interference (MMI) couplers. A 3x3 planar optical waveguide coupler is analyzed by the coupled mode theory and the other can be analyzed by using the self-imaging theory [14].

As an example, 3x3 planar directional coupler and 3x3 MMI coupler have been investigated in Figure 4 and 5. The silicon waveguide is used for the simulations. The waveguide has a standard silicon thickness of $h_{co} = 220\text{nm}$ and access waveguide widths are $W_a = 0.5\ \mu\text{m}$ for single mode operation. It is assumed that the designs are for the TE polarization at a central optical wavelength $\lambda = 1550\text{nm}$.

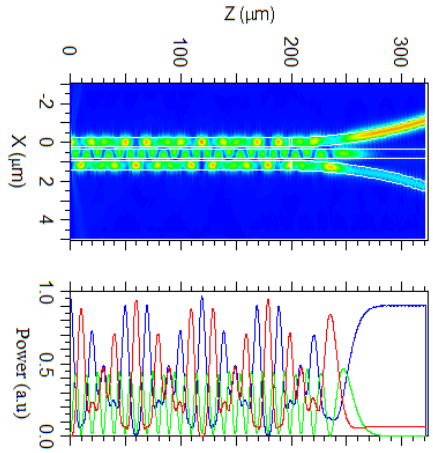

(a) Gap between two adjacent waveguide g=100nm

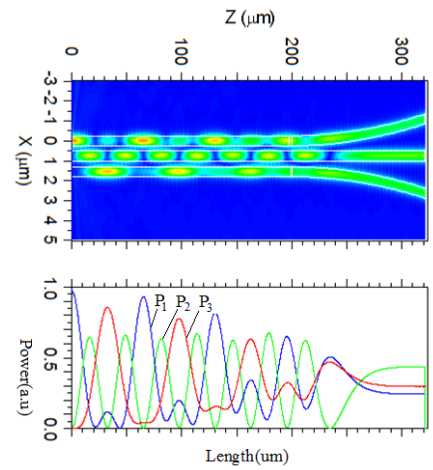

(b) Gap between two adjacent waveguide g=300nm

Figure 4. *Simulations of a 3x3 planar directional coupler*

The coupler consists of three optical waveguides with their centers aligned in the same plane. It is assumed that the coupling exists only between the neighboring pairs of waveguides. The coupling characteristics can be obtained by using the mode coupling theory. Complex amplitudes a_i of the fields inside three waveguides are governed by a set of differential equations [7]

$$\begin{pmatrix} \frac{da_1}{dz} \\ \frac{da_1}{dz} \\ \frac{da_1}{dz} \end{pmatrix} = \begin{pmatrix} 0 & j\kappa_{12} & 0 \\ j\kappa_{21} & 0 & j\kappa_{23} \\ 0 & j\kappa_{32} & 0 \end{pmatrix} \begin{pmatrix} a_1 \\ a_2 \\ a_3 \end{pmatrix} \quad (16)$$

Solving (16) with $\kappa = \kappa_{ij}$ $(i, j = 1 \div 3)$ being coupling coefficients between the waveguide *i* and *j*, the output field amplitudes of the 3x3 coupler are given by

$$\begin{pmatrix} b_1 \\ b_2 \\ b_3 \end{pmatrix} = \begin{pmatrix} \tau & -j\frac{1}{\sqrt{2}}\kappa & -j\frac{1}{\sqrt{2}}\kappa \\ -j\frac{1}{\sqrt{2}}\kappa & \frac{1}{2}(\tau+1) & \frac{1}{2}(\tau-1) \\ -j\frac{1}{\sqrt{2}}\kappa & \frac{1}{2}(\tau-1) & \frac{1}{2}(\tau+1) \end{pmatrix} \begin{pmatrix} a_1 \\ a_2 \\ a_3 \end{pmatrix} \quad (17)$$

where $\tau = \cos(\sqrt{2}kz)$, and $\kappa = \sin(\sqrt{2}kz)$ are transmission and coupling coefficients, $k = \frac{2\pi}{\lambda}$ is the wave number, z is the coupling length.

Substituting (17) into (8), (9) and (10), (11), the transmitted power at the output port in the two cases can be expressed by

Input port $a_1 = 1$ *(normalized)*

$$P_1 = \frac{1}{4} \cdot \frac{(1+\tau)^2 + 4\alpha^2\tau^2 - 4\alpha(1+\tau)\tau\cos(\varphi)}{1 + 0.25\alpha^2(1+\tau)^2 - \alpha(1+\tau)\cos(\varphi)} \quad (18)$$

$$P_2 = \frac{1}{2} \cdot \frac{(1-\tau^2)[1+\alpha^2 - 2\alpha\cos(\varphi)]}{1 + 0.25\alpha^2(1+\tau)^2 - \alpha(1+\tau)\cos(\varphi)} \quad (19)$$

Input port $a_2 = 1$ *(normalized)*

$$P_3 = \frac{1}{2} \cdot \frac{(1-\tau^2)[1+\alpha^2 - 2\alpha\cos(\varphi)]}{1 + 0.25\alpha^2(1+\tau)^2 - \alpha(1+\tau)\cos(\varphi)} \quad (20)$$

$$P_4 = \frac{1}{4} \cdot \frac{\alpha^2(1+\tau)^2 + 4\tau^2 - 4\alpha(1+\tau)\tau\cos(\varphi)}{1 + 0.25\alpha^2(1+\tau)^2 - \alpha(1+\tau)\cos(\varphi)} \quad (21)$$

and the power at output port 3:

$$P_5 = \frac{1-\tau^2}{2(1 + 0.5\alpha^2(1+\tau)^2 - \alpha(1+\tau)\cos(\varphi))} \quad (22)$$

At resonance, $\varphi = 2\pi m$, where m is some integer, the above equations are rewritten as follows

$$P_1 = \frac{1}{4} \cdot \frac{[(1+\tau) - 2\alpha\tau]^2}{[1 - 0.5\alpha(1+\tau)]^2} \quad (23)$$

$$P_2 = \frac{1}{2} \cdot \frac{(1-\tau^2)(1-\alpha)^2}{[1 - 0.5\alpha(1+\tau)]^2} \quad (24)$$

$$P_3 = \frac{1}{2} \cdot \frac{(1-\tau^2)(1-\alpha)^2}{[1 - 0.5\alpha(1+\tau)]^2} \quad (25)$$

$$P_4 = \frac{1}{4} \cdot \frac{[\alpha(1+\tau) - 2\tau]^2}{[1 - 0.5\alpha(1+\tau)]^2} \quad (26)$$

It should be noted that $P_2 = P_3$ and its value will vanish only when $\tau = \pm 1$ or $\alpha = 1$ (lossless case, i.e. there is no optical loss inside the ring resonator). Therefore, these ports will not be used in our analysis.

From (26), it shows that for the case input signal at port 2, the transmitted power at output port 2 vanishes, i.e. $P_4 = 0$, when the relation between the coupling coefficient τ and the internal loss α meets the condition: $\tau = \frac{\alpha}{2-\alpha}$. This is also the critical condition of the resonator.

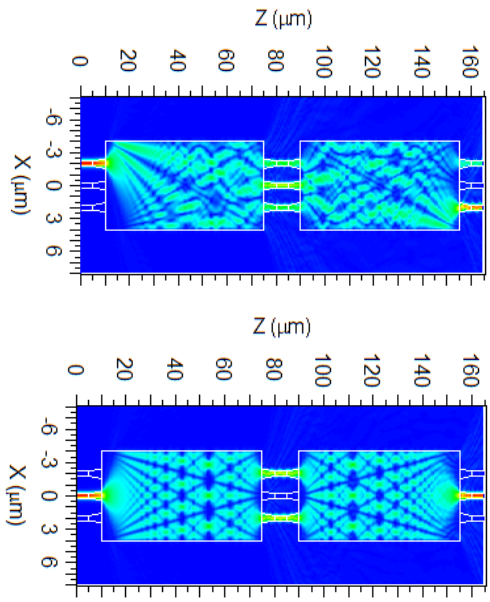

Figure 5. *Simulations of a 3x3 MMI cascaded coupler*

Figure 6 shows the power transmission characteristics P_3 against the internal loss α for a given value of the coupling length *kz*. The dependence of the transmission on α near the critical coupling is particularly significant. Small changes in α for a given τ, or vice versa, can control the transmitted power, between unity and zero. If we can learn how to control α and/or τ, we have a basis for a switching technology. If we can do it sufficiently rapidly, we have the basis of a new type of an optical modulator. At a constant value of the internal loss, if we can make the coupler operating near the critical coupling point then switching functions can be achieved from this characteristic.

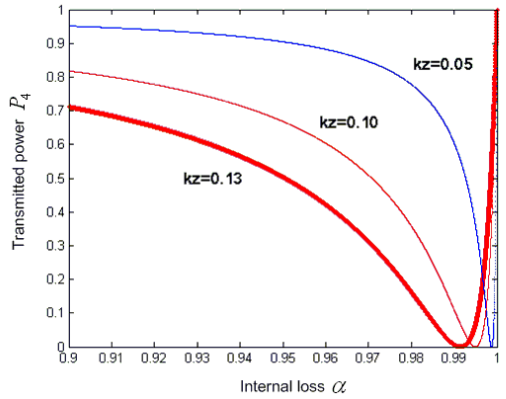

Figure 6. *Transmitted power at the output port 2, P_3against the internal loss∝ at a variety of the coupling lengths kz=0.05, 0.10, and 0.13*

Figure 7 shows the transmission characteristics against frequency near critical coupling for a given value *kz=0.13* ($\tau = 0.9958$). The device is designed on Silicon on Insulator (SOI) technology. Optical waveguides supports only one mode with the effective refractive index $n_{eff} = 3.4767$ calculated from the Finite Difference Method (FDM)[15]. Ring resonator has a radius $R = 300\mu m$ large enough to reduce the bending loss. The simulations are carried out for four different values of the internal loss $\alpha = 0.99$, *1.0, 1.005,* and *1.0085.* A gain is concluded in the ring resonator to have $\alpha > 1$. In this case, the transmitted power is amplified. An important characteristic of this resonator is that the resonance peak can be made arbitrarily narrow. When $\alpha = 2/(1+\tau)$, according to (25), the transmission reaches infinite value. This means that laser oscillation is obtained.

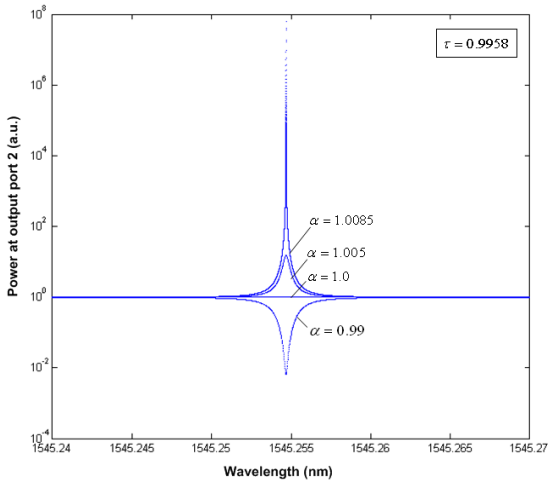

Figure 7. *Transmitted power at the output port 2 , P_3 against wavelength at different value of the internal loss ∝= 0.99, 1.0, 1.005, and $\alpha = 1.0085$. The figure shows the transmission near a resonance wavelength $\lambda = 1545.223nm$*

Some performance parameters of the resonator are Finesse, Q-factor, resonance width, and bandwidth. These are all terms that are mainly related to the full width at half of the maximum (FWHM) of the transmission. The FWHM of the micro-ring resonance is the resonance width or the bandwidth and can be calculated from (27) below.

$$P_5 = \frac{T_{max}}{1 + F\sin^2(\varphi/2)} \tag{27}$$

$$\delta\lambda_{FWHM} = \frac{[\alpha(1+\tau)-2]\lambda^2}{\pi n_{eff} L\sqrt{2\alpha(1+\tau)}} \tag{28}$$

where $T_{max} = \frac{2(1-\tau^2)}{[\alpha(1+\tau)-2]^2}$, $F = \frac{8\alpha(1+\tau)}{[\alpha(1+\tau)-2]^2}$, and L is the circumference of the ring.

The Free Spectral Range (FSR) is the distance between two peaks on a wavelength scale. By differentiating the equation $\varphi = \beta L$, we get $FSR = \frac{\lambda^2}{n_g L}$, where the group index is $n_g = n_{eff} - \lambda\frac{dn_{eff}}{d\lambda}$.

The Finesse F is defined as the ratio of the FSR and the bandwidth and thus can be calculated by $F = \frac{FSR}{\delta\lambda_{FWHM}}$. Moreover, The Q-factor is defined as the ratio of the wavelength of the peak to the FWHM of the peak, $Q = \frac{\lambda}{\delta\lambda_{FWHM}}$.

For the case input signal at port 1, the power at output port 1 is calculated from (23). The power P_1 vanishes only if $\tau = \tau_1 = 1/(2\alpha - 1)$ and the power P_1 reaches infinite value with $\tau = \tau_2 = (2-\alpha)/\alpha$. This may be one of the most interesting characteristics of the ring resonator because for a given value of the internal loss or gain α, the difference between the values of τ_1 and τ_2 is very small. Therefore, a very low power switch can be made from this configuration by using thermo-optic, or electro-optic effects.

4. Conclusion

We have presented a universal analysis for micro-ring resonators using 3x3 couplers. Expressions for the output intensities for the ring resonator based on any kind of 3x3 couplers are derived. The transmission characteristics of a ring resonator designed on SOI technology as well as the performance parameters including the free spectral range, finesse, and Q-factor are studied. The switching, modulation and laser oscillation functions have been realized. It shows that these resonators will be very promising passive and active components for photonic integrated circuits in the future.

Acknowledgements

This research is funded by Vietnam National Foundation for Science and Technology Development (NAFOSTED) under grant number “103.02-2013.72" and Vietnam National University, Hanoi (VNU) under project number QG.15.30.

REFERENCES

[1] Ioannis Chremmos, Otto Schwelb, and Nikolaos Uzunoglu (Editors), *Photonic Microresonator Research and Applications*: Springer, 2010.

[2] Trung-Thanh Le, "Microring resonator Based on 3x3 General Multimode Interference Structures Using Silicon Waveguides for Highly Sensitive Sensing and Optical Communication Applications," *International Journal of Applied Science and Engineering*, vol. 11, pp. 31-39, 2013.

[3] T. T Le and L. W Cahill, "Microresonators Based on 3x3 Multimode Interference Couplers on an SOI Platform," in *The 2009 Annual Meeting of the IEEE Lasers & Electro-optics Society (LEOS)*, Belek-Antalya, Turkey, 4-8 Oct. 2009.

[4] J. M. Choi, R. K. Lee, and A. Yariv, "Control of critical coupling in a ring resonator–fiber configuration: application to wavelength-selective switching, modulation, amplification, and oscillation," *Optic Letters*, vol. 26, pp. 1236-1238, 2001.

[5] A. Yariv, "Critical coupling and its control in optical waveguide-ring resonator systems," *IEEE Photonics Technology Letters*, vol. 14, pp. 483-485, 2002.

[6] S.K. Sheem, "Optical Fiber Interferometers with 3x3 Directional Couplers: Analysis," *Journal of Applied Physics*, vol. 52, pp. 3865-3872, June 1981.

[7] Y. H. Chew, Tjeng T. Tjhung, and F. V. C Mendis, "Performance of single-and double-ring resonators using 3 x 3 optical fiber coupler," *Journal of Lightwave Technology*, vol. 11, pp. 1998-2008, 1993.

[8] Xiaobei Zhang, Dexiu Huang, and Xinliang Zhang, "Transmission characteristics of dual microring resonators coupled via 3×3 couplers," *Optics Express*, vol. 15, pp. 13557-13573, 2007.

[9] Chao Ying Zhao and Wei Han Tan, "Transmission performance of one waveguide and double micro-ring resonator using 3×3 optical fiber coupler," *Journal of Modern Optics*, vol. 63, pp. 1726-1733, 2016.

[10] Xiaobei Zhang, Dexiu Huang, and Xinliang Zhang, "Transmission characteristics of dual microring resonators coupled via 3x3 couplers," *Optics Express*, vol. 17, pp. 13557-73, 2007.

[11] Trung-Thanh Le, " Arbitrary Power Splitting Couplers Based on 3x3 Multimode Interference Structures for All-optical Computing," *International Journal of Engineering and Technology, Singapore*, vol. 3, pp. 565-569, 2011.

[12] Trung-Thanh Le, "Arbitrary Power Splitting Couplers Based on 3x3 Multimode Interference Structures for All-optical Computing," *International Journal of Engineering and Technology, Singapore*, vol. 2, pp. 565-569, 2011.

[13] A. Yariv, "Universal relations for coupling of optical power between microresonators and dielectric waveguides," *Electronics Letters*, vol. 36, pp. 321–322, 2000.

[14] M. Bachmann, P. A. Besse, and H. Melchior, "General self-imaging properties in N x N multimode interference couplers including phase relations," *Applied Optics*, vol. 33, pp. 3905-, 1994.

[15] Lê Trung Thành, Nguyen Canh Minh, Nguyen Van Khoi *et al.*, "Design of silicon wires based directional couplers for microring resonators," *Journal of Science and Technology, University of Danang*, vol. 11, 2015.

(The Board of Editors received the paper on 10/4/2017, its review was completed on 04/5/2017)